AD-A065 898 AIR FORCE AERO PROPULSION LAB WRIGHT-PATTERSON AFB OHIO F/G 20/13
EXPERIMENTAL INVESTIGATION OF HEAT TRANSFER TO A THREADED CYLIN--ETC(U)
JAN 78 P J HENDERSON

UNCLASSIFIED AFAPL-TR-78-1 NL

END
DATE FILMED
5-79
DDC

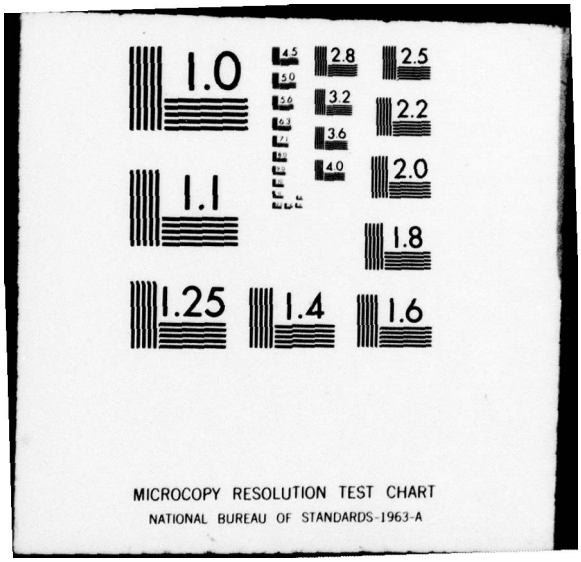
1.0
1.1
1.25
1.4
1.6
1.8
2.0
2.2
2.5
2.8
3.2
3.6
4.0
4.5
5.0
5.6
MICROCOPY RESOLUTION TEST CHART
NATIONAL BUREAU OF STANDARDS-1963-A

AFAPL-TR-78-1

LEVEL II

AD A065898

EXPERIMENTAL INVESTIGATION OF HEAT TRANSFER TO A THREADED CYLINDER IN CROSSFLOW

COMPONENTS BRANCH
TURBINE ENGINE DIVISION

JANUARY 1978

TECHNICAL REPORT AFAPL-TR-78-1
Final Report for Period March 1977 to August 1977

AIR FORCE AERO PROPULSION LABORATORY
AIR FORCE WRIGHT AERONAUTICAL LABORATORIES
AIR FORCE SYSTEMS COMMAND
WRIGHT-PATTERSON AIR FORCE BASE, OHIO 45433

NOTICE

When Government drawings, specifications, or other data are used for any purpose other than in connection with a definitely related Government procurement operation, the United States Government thereby incurs no responsibility nor any obligation whatsoever; and the fact that the government may have formulated, furnished, or in any way supplied the said drawings, specifications, or other data, is not to be regarded by implication or otherwise as in any manner licensing the holder or any other person or corporation, or conveying any rights or permission to manufacture, use, or sell any patented invention that may in any way be related thereto.

This report has been reviewed by the Information Office (OI) and is releasable to the National Technical Information Service (NTIS). At NTIS, it will be available to the general public, including foreign nations.

This technical report has been reviewed and is approved for publication.

Allen E. Hause

ALLEN E. HAUSE
Project Engineer
Components Branch
Turbine Engine Division

Wayne A. Tall

WAYNE A. TALL
Tech Area Manager, Turbines
Components Branch
Turbine Engine Division

FOR THE COMMANDER

Marvin A. Stibich

MARVIN A. STIBICH
Acting Chief
Components Branch
Turbine Engine Division

"If your address has changed, if you wish to be removed from our mailing list, or if the addressee is no longer employed by your organization please notify AFAPL/TBC *,W-PAFB, OH 45433 to help us maintain a current mailing list".*

Copies of this report should not be returned unless return is required by security considerations, contractual obligations, or notice on a specific document.

AIR FORCE/56780/7 July 1978 — 50

UNCLASSIFIED

SECURITY CLASSIFICATION OF THIS PAGE (When Data Entered)

REPORT DOCUMENTATION PAGE	READ INSTRUCTIONS BEFORE COMPLETING FORM
1. REPORT NUMBER: AFAPL-TR-78-1	2. GOVT ACCESSION NO. / 3. RECIPIENT'S CATALOG NUMBER
4. TITLE (and Subtitle): EXPERIMENTAL INVESTIGATION OF HEAT TRANSFER TO A THREADED CYLINDER IN CROSSFLOW.	5. TYPE OF REPORT & PERIOD COVERED: FINAL REPORT. MARCH 1[illegible]—AUGUST [illegible]77.
	6. PERFORMING ORG. REPORT NUMBER
7. AUTHOR(s): Philip James Henderson	8. CONTRACT OR GRANT NUMBER(s)
9. PERFORMING ORGANIZATION NAME AND ADDRESS: Air Force Aero Propulsion Laboratory (AFAPL/TBC) Air Force Wright Aeronautical Laboratories Wright-Patterson Air Force Base, Ohio 45433	10. PROGRAM ELEMENT, PROJECT, TASK AREA & WORK UNIT NUMBERS: P.E. 62203F, Proj 3066 Task 306606, W.U. 30660634
11. CONTROLLING OFFICE NAME AND ADDRESS: 57p.	12. REPORT DATE: January [illegible]978 / 47
14. MONITORING AGENCY NAME & ADDRESS(if different from Controlling Office)	15. SECURITY CLASS. (of this report): UNCLASSIFIED
	15a. DECLASSIFICATION/DOWNGRADING SCHEDULE

16. DISTRIBUTION STATEMENT (of this Report)

APPROVED FOR PUBLIC RELEASE; DISTRIBUTION UNLIMITED.

17. DISTRIBUTION STATEMENT (of the abstract entered in Block 20, if different from Report)

18. SUPPLEMENTARY NOTES

19. KEY WORDS (Continue on reverse side if necessary and identify by block number)

Heat Flux
Cylinder in Crossflow
Surface Roughness
Hydrogen
Stagnation Line

20. ABSTRACT (Continue on reverse side if necessary and identify by block number)

An experimental investigation of heat transfer to cylinders in crossflow was conducted at the Hydrogen Heat Transfer Facility of the Air Force Aero Propulsion Laboratory. The heat transfer at the stagnation line of a cylinder with circumferential threads, 0.010 inches deep and 0.015 inches wide, was compared with the heat transfer to a smooth cylinder. The investigation covered the Reynolds Number ranges of 38,000 to 118,000. A hollow cylinder (1.25 inches OD) was instrumented with foil heat flux sensors and fixed behind a hydrogen combustor. Gas temperatures did not exceed 1060°R.

DD FORM 1 JAN 73 1473 EDITION OF 1 NOV 65 IS OBSOLETE

UNCLASSIFIED

SECURITY CLASSIFICATION OF THIS PAGE (When Data Entered)

011 570 LB

The investigation showed that the heat transfer to the stagnation line of the threaded cylinder was significantly different from the heat transfer to the smooth cylinder. Below Re_D = 83,000, the smooth cylinder had the greater heat flux. Above Re_D = 88,000, the threaded cylinder had the greater heat flux. Between Re_D = 83,000 and Re_D = 88,000, a sudden shift in the heat transfer took place for both cylinders, probably corresponding to the development of a turbulent boundary layer.

FOREWORD

This final report was submitted by Phillip Henderson in partial fulfillment of the requirements for the degree Master of Science jointly sponsored by the Ohio State University and the Air Force Aero Propulsion Laboratory, Air Force Systems Command, Wright-Patterson Air Force Base, Ohio, under Project Number 3066, Task 306606, and Work Unit 30660634 with Captain John A. Vonada (AFAPL/TBC) as the project engineer.

The author wishes to acknowledge the following people: thesis advisor, Dr. Lit S. Han, Professor of Mechanical Engineering, the Ohio State University; Allan Hause, Captain John A. Vonada, and Wayne Tall of the Air Force Aero Propulsion Laboratory, for the use of the facility, technical guidance, and long hours spent in support of this O.S.U graduate program; Bernard DeWinter and Dennis Shutts of the Aero Propulsion Laboratory for efforts in installing and testing the experimental apparatus; and the craftsmen of the Propulsion Laboratory's machine and instrumentation shops for their contributions to this study.

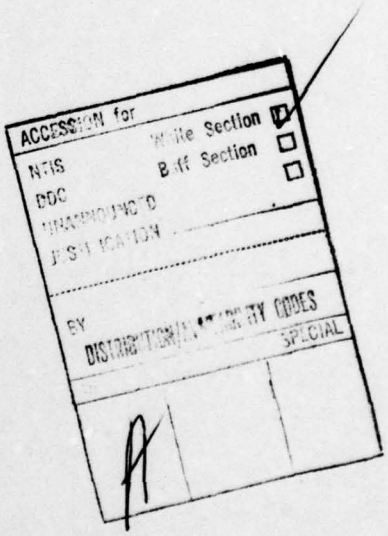

TABLE OF CONTENTS

LIST OF ILLUSTRATIONS

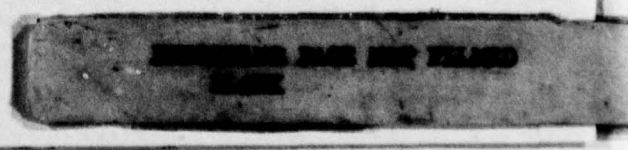

LIST OF TABLES

NOMENCLATURE

A_t	Cross-sectional area of gas path
Cp	Specific heat at constant pressure
D	Cylinder diameter
h	Convective heat transfer coefficient
HF	Millivolt output from heat flux sensor
HFCF	Heat flux correction factor for temperature
k_g	Thermal conductivity of gas
k_s	Height of surface roughness
k_w	Thermal conductivity of wall
$\dot{m}$	Gas mass flow rate
M	Free stream Mach number
Nu	Nusselt number, hD/k_g
P_g	Free stream gas pressure (absolute)
Pr	Prandtl number, $Cp\mu/k_g$
q	Heat flux
q_{cond}	Heat flux by conduction
q_{conv}	Heat flux by convection
Re_D	Reynolds number, $\rho U_g D/\mu$
s	Standard deviation
T	Temperature
T_g	Free stream gas temperature

NOMENCLATURE (Cont'd.)

$T_{w,i}$	Inside wall temperature
$T_{w,o}$	Outside wall temperature
u'	Fluctuating component of gas velocity
U_g	Free stream gas velocity
x	Wall thickness
δ	Boundary layer thickness
ε	Turbulence intensity
ρ	Gas density
μ	Gas viscosity

I. INTRODUCTION

Research in turbine airfoil production techniques has demonstrated the feasibility of photoengraving an airfoil cross section with complex internal cooling passages on thin metal sheets (approximately 0.010 inches thick). The thin airfoil sections are bonded together to form a laminated turbine vane. Stacking tolerances cause a slight misalignment of the laminate sections. Without a final machining process to smooth the outer surface of the bonded airfoils, the mis-aligned laminates produce a surface roughness parallel to the flow direction. Since the final cost of a metallic component is directly related to the number of machining operations, a cost savings is realized if the surface roughness is not removed.

The purpose of this study was to investigate experimentally the effect on heat transfer of surface roughness parallel to the flow. A cylinder was used to represent the leading edge of a turbine vane and the investigation was limited to the stagnation region.

Many previous investigators have dealt with surface roughness effects on heat transfer. Most, however, are concerned with either two-dimensional elements (e.g., sand

roughness) or one-dimensional grooves and trip wires perpendicular to the flow. Of the references reviewed, none were directly concerned with one-dimensional roughness parallel to the flow. This type of surface could possibly be considered as finned, but the question remains: Does the roughness parallel to the flow affect the heat transfer to the surface in the turbulent environment of a turbine combustor?

Owen and Thomson (Ref 1:322)*, in a study of surface roughness effects, suggest that eddies in the flow along a rough surface penetrate the region between the roughness protrusions, scour the wall, and return to the main stream. In turbulent flow, any additional disturbances created by the roughness join those already present. This would increase the heat flux.

Roughness can be characterized several ways. A relative roughness for a flat surface is given by Schlichting: k_s/δ, where k_s is the size of the roughness protrusion and δ is the boundary layer thickness (Ref 2:610). Another characterization, used during a study of drag loss coefficient versus sand roughness of turbine blade surfaces, was to compare the roughness height to the chord length of the airfoil (Ref 2:618). Schlichting (Ref 2: 615) refers to the

*Number following colon refers to page number in reference.

"admissible roughness" as "that maximum height of individual roughness elements which causes no increase in drag compared with a smooth wall." This definition of admissible roughness refers to heat transfer effects as well as roughness induced drag.

For a cylinder in laminar crossflow, the Nusselt number at the stagnation line can be correlated by

$$Nu = 2\,A(Pr)\,(Re_D)^{\frac{1}{2}}$$

A table for A(Pr) is given in Schlicting (Ref 2:290). For Pr = 0.7 (air), A(Pr) = 0.495. This gives the approximation that

$$Nu = (Re_D)^{\frac{1}{2}}$$

Using $Nu = h_g D / k_g$ and $Re_D = U_g D \rho / \mu$

it follows that $$h_g = \frac{k_g}{D}\left[\frac{U_g D \rho}{\mu}\right]^{\frac{1}{2}}$$

Turbulence intensity, ε, is given by

$$\varepsilon = \frac{\left[\overline{(u')^2}\right]^{\frac{1}{2}}}{\overline{U}_g}$$

where u' is the fluctuating component of the free stream velocity. The value of the turbulence intensity has a well noted effect on heat transfer to cylinders in crossflow.

Primarily, it causes a shift in the transition and separation points, but turbulence also affects the local heat flux. Some researchers have noted that experiments at the same Reynolds number show differing results (Ref 3,4,&5). This is thought to be caused by varying free stream turbulence.

Smith and Kuethe (Ref 3) have shown that a turbulence intensity of 6% will cause a 70% increase in stagnation line heat transfer as compared to laminar flow (Re_D = 240,000). Their study also noted a wide disparity of results of previous researchers. From their work in low speed wind tunnels, they have suggested a linear relation between the stagnation-line Nusselt number and the free stream turbulence at a constant Reynolds number. At a Reynolds number of 60,000, they report the ratio of $Nu / (Re_D)^{\frac{1}{2}}$ rising from about 1.0 at a free stream turbulence of 0.1% to 1.3 at a free stream turbulence of 5%. At a Reynolds number of 120,000, $Nu / (Re_D)^{\frac{1}{2}}$ is approximately 1.5 for 5% turbulence. Their work could help to explain the data scatter found in this study.

Dils and Follansbee (Ref 5) made the first reported direct measurements of convection coefficients of small cylinders in the crossflow of a combustor exhaust gas environment. Although their study was limited to Reynolds numbers between 4000 and 20,000, the combustion environment used is similar to this study. They showed that stagnation

line heat transfer coefficients are higher than values obtained in low turbulence cold gas streams of comparable Reynolds numbers. The major portion of their work was the investigation of gas stream fluctuations measured by fast response thermocouples mounted to the outer wall of a cylinder. The fast response instrumentation indicated peak to peak temperature fluctuations of 20% to 100% of the average free stream temperature. Similar temperature fluctuations in this study may explain the data scatter shown later.

As a result of the work of Dils and Follansbee, an empirical relation was determined to relate Nusselt and Reynolds numbers:

$$Nu = 1.40\ (Re_D)^{\frac{1}{2}} \qquad (Re_D = 4000 - 20{,}000)$$

Their correlation was determined for cylinders in the exhaust gas environment of a low injection pressure combustor where turbulence level ranged from 8% to 15%. The correlation will be compared to the data from this study in Section IV.

In this study, an instrumented, air-cooled, hollow cylinder was used to represent the leading edge of a turbine airfoil. A hydrogen combustor facility was used to generate conditions approximating a turbine engine combustor. Heat flux measurements were determined by thin, heat flux sensors and thermocouples operating in steady state conditions. By knowing the material properties and the gas path conditions,

the relationship between the Nusselt number and the Reynolds number was obtained.

Initial tests were made with circumferential threads on the cylinder. The outer surface was then machined smooth with the instrumentation in place. Previous test conditions were repeated with the smooth surfaced cylinder and the results compared. Unfortunately, test cell scheduling limited the investigation to one rough surfaced cylinder and one smooth surfaced cylinder.

Descriptions of the apparatus used, the conditions tested (Re_D = 38,000 to 118,000), and the results and conclusions of this work are presented in the following sections.

II. EXPERIMENTAL APPARATUS

Test Facility

The Air Force Aero Propulsion Laboratory (AFAPL) Hydrogen Heat Transfer Facility located at Wright-Patterson Air Force Base was used for this investigation. This facility was developed by AFAPL to test turbine vane cooling configurations (Ref 6&7).

Figure 1 shows the AFAPL Hydrogen Heat Transfer Facility. Figure 2 shows the control room which is isolated from the combustor. Hydrogen is used as fuel because of the well defined radiation characteristics of the principal product of combustion, water vapor. The combustor is capable of temperatures up to 4260 ^{o}R with a maximum mass flow rate of air of 6 lbm/sec at 50 psia. Hydrogen is injected into the airstream 48 inches from the test section where vane specimens are mounted in the throat of a convergent-divergent nozzle (Figure 3).

Hydrogen flow rate is measured by a Herschel venturi tube in the supply line. A differential pressure transducer, a thermocouple and a second pressure transducer give flow and upstream hydrogen source conditions.

Mass flow rate of air is controlled by upstream

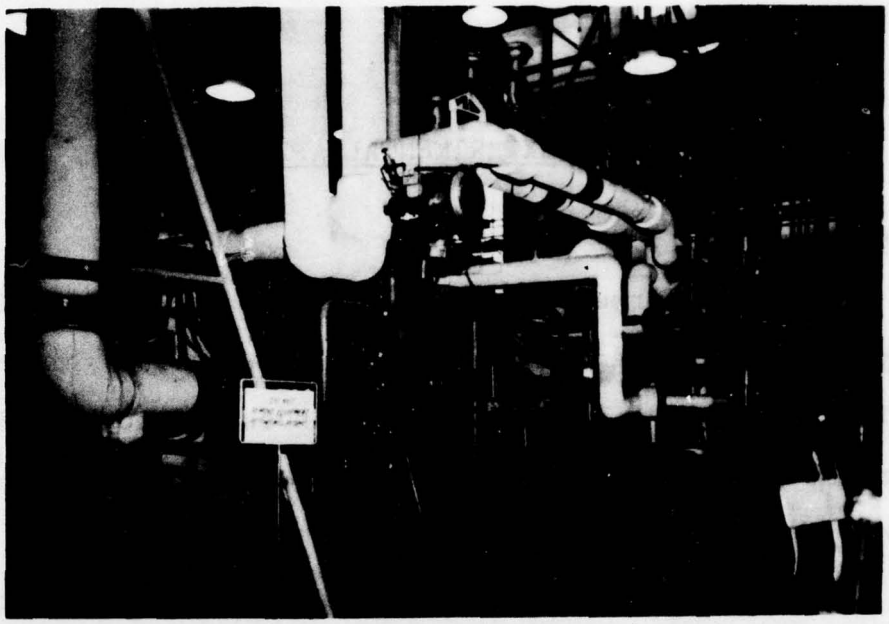

Fig 1. AFAPL Hydrogen Heat Transfer Facility
(Courtesy of AFAPL/TBC)

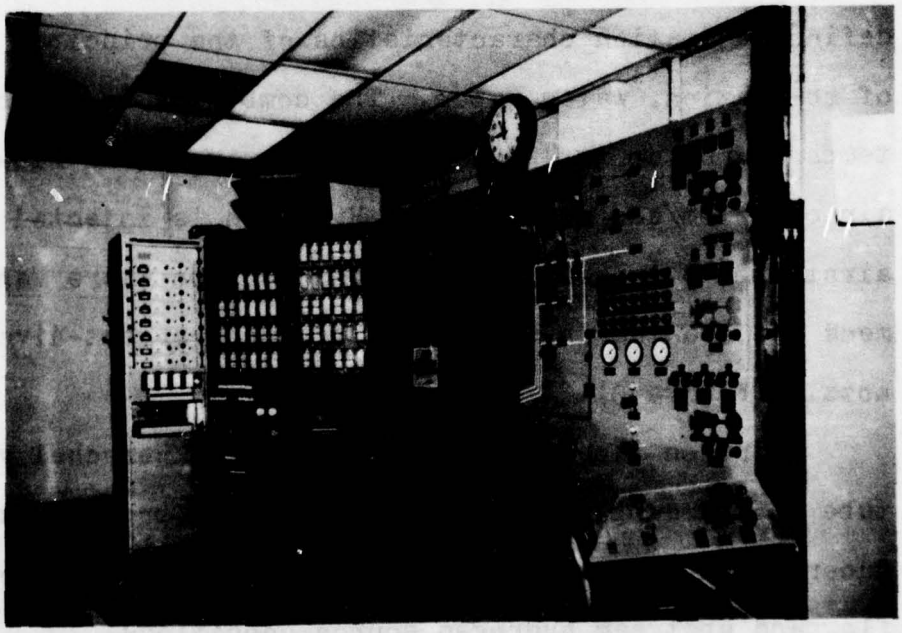

Fig 2. Facility Control Room
(Courtesy of AFAPL/TBC)

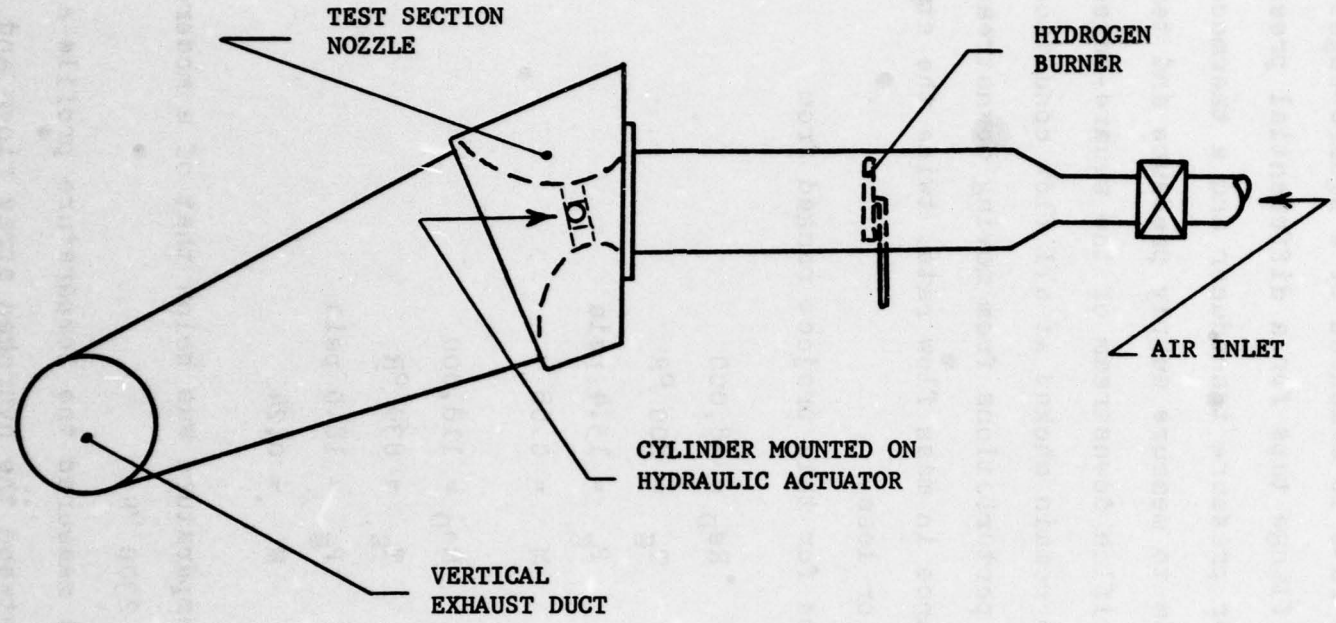

Fig 3. Layout of hydrogen combustor (top view)

pressure. The flow rate is measured by a square-edged orifice plate with flange taps for a differential pressure transducer. Another pressure transducer and a thermocouple are located upstream to measure supply pressure and temperature. A second orifice downstream of the square-edged orifice is sized to remain choked at all flow conditions and prohibits pressure perturbations from moving downstream. The measured tolerance in mass flow rate, twice the standard deviation, is $\pm$ 2% or less.

Test conditions for this project ranged from

Re_D = 38,000
T_g = 800 ^oR
P_g = 15.4 psia
M = 0.08

to

Re_D = 118,000
T_g = 839 ^oR
P_g = 18.0 psia
M = 0.24

The range of gas temperature was below that of a modern gas turbine, typically 2300 ^oR.

Vonada (Ref 7) measured the temperature profile at several stations between the hydrogen spray rings and the nozzle. His data show that a nearly uniform temperature

pattern exists with the maximum gradients near the chamber walls. The study by Vonada was limited to gas temperatures above 1460 ^{o}R at mass flow rates above 0.8 lbm/sec. Since low temperature measurements were not available, the same flow uniformity was assumed for this investigation.

The test section nozzle is a rectangular area of 16.7 square inches. This nozzle is designed to turn the flow approximately 80^{o} to accommodate a set of turbine vanes (Figure 4). The upstream pipe leading from the hydrogen injection rings has a circular cross section of about 9 inches diameter (66 square inches). The length of the convergent nozzle is 8 inches.

The facility was fitted with a pneumatic actuator system to insert the test cylinder into the gas path. This was a necessary feature because of the unpredictable nature of the burner during the initiation of combustion. Each flow condition was established before the cylinder was inserted into the hot gas.

Test Specimen

The test cylinder (304 stainless steel tubing - 1.25 inches OD) is shown in Figure 5.

A sample of laminated turbine airfoil was measured with a microscope to determine the surface roughness. The measurement revealed that a rectangular thread 0.010 inches deep and 0.015 inches wide would approximate the airfoil

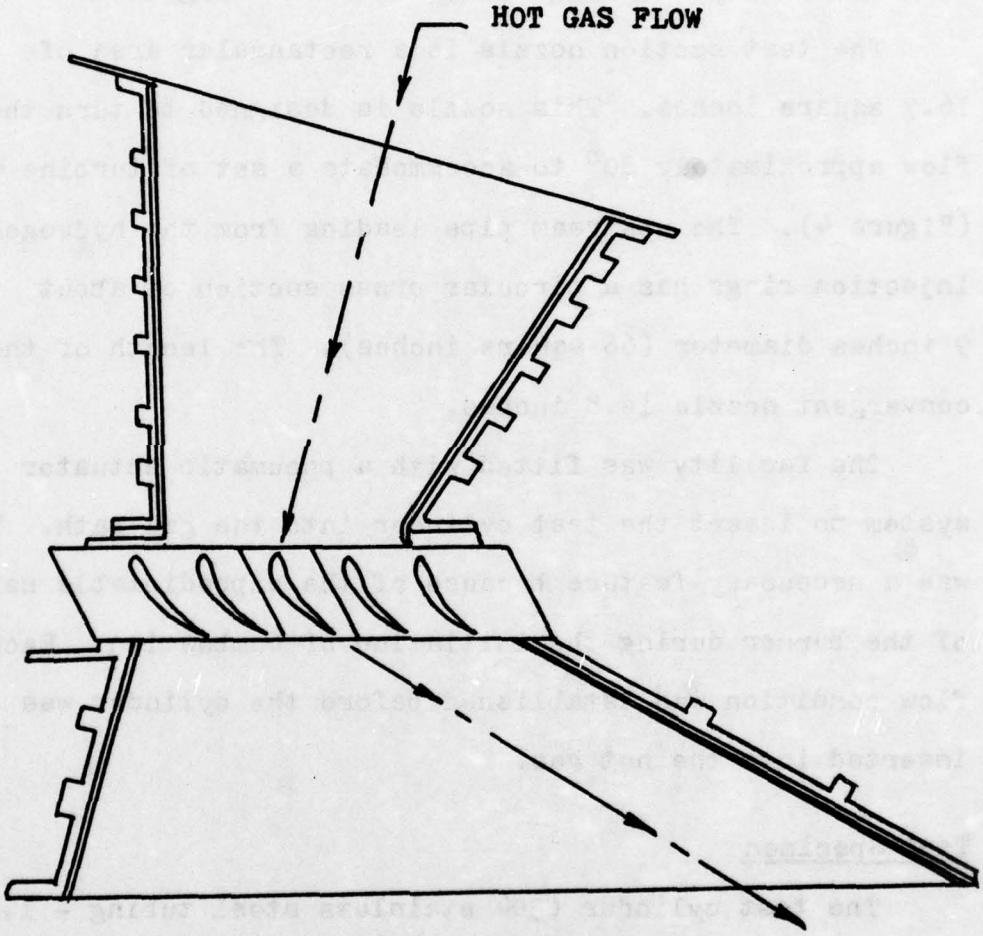

Fig 4. Combustor rig nozzle (top view)

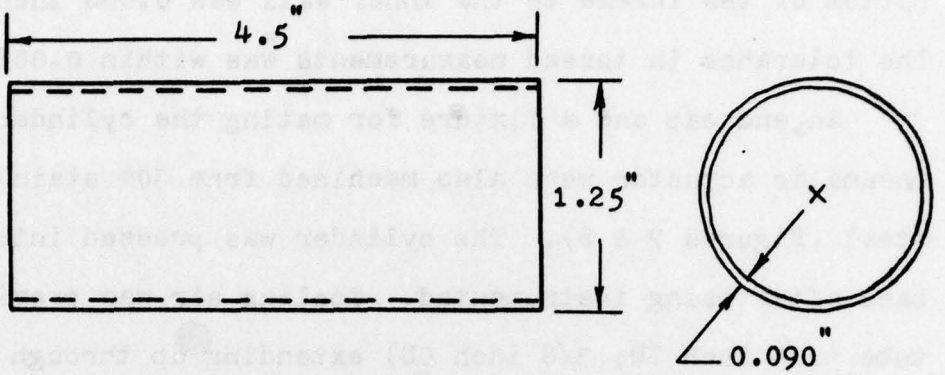

Fig 5. Test Cylinder

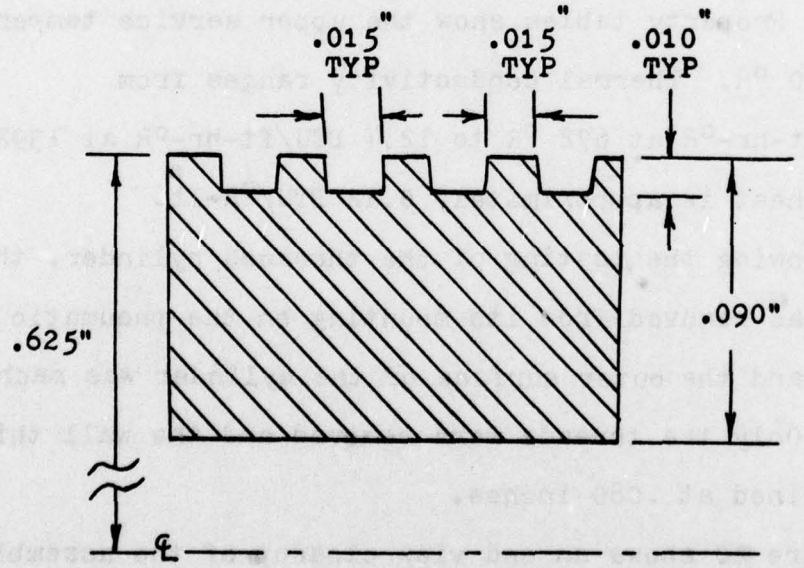

Fig 6. Wall section showing thread size

surface (Figure 6). The final wall thickness from the bottom of the thread to the inner wall was 0.080 inches. The tolerance in thread measurements was within 0.001 inches.

An end cap and a fixture for mating the cylinder to the pneumatic actuator were also machined from 304 stainless steel (Figures 7 & 8). The cylinder was pressed into the base after being instrumented. Cooling air was provided by a tube (1/4 inch ID; 3/8 inch OD) extending up through the fixture base and impinging air on the inside of the end cap. Holes in the fixture base allowed for cooling air escape as well as routes for instrumentation leads (Figure 9).

Stainless steel (304) was used because of its availability. Property tables show the upper service temperature to be 2160 ^{o}R. Thermal conductivity ranges from 9.4 BTU/ft-hr-^{o}R at 672 ^{o}R to 12.4 BTU/ft-hr-^{o}R at 1392 ^{o}R. Specific heat is approximately 0.12 BTU/^{o}R-lb.

Following the testing of the threaded cylinder, the fixture was removed from its mounting on the pneumatic actuator and the outer surface of the cylinder was machined smooth. Only the threads were removed and the wall thickness remained at .080 inches.

Figure 10 shows an end view closeup of the assembled, threaded cylinder. Figure 11 shows the assembled and instrumented cylinder installed on the pneumatic actuator. Figure 12 shows the actuator installed in the underside of the hydrogen combustor exhaust duct.

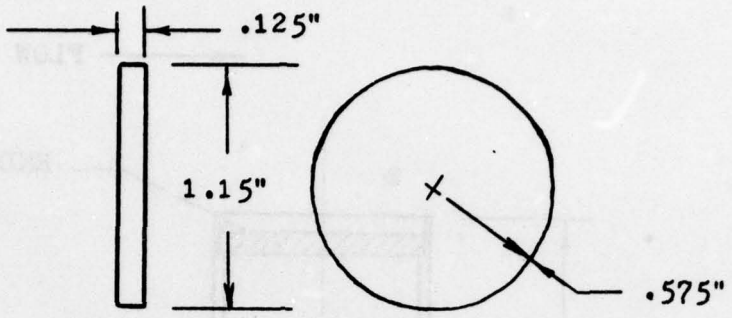

Fig 7. End cap

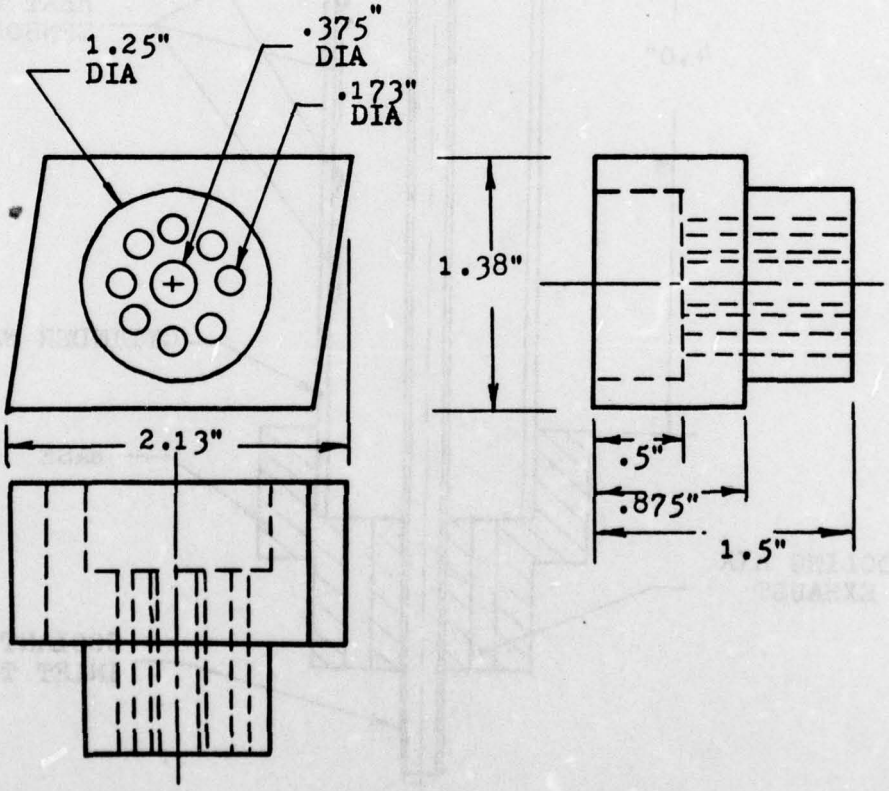

Fig 8. Fixture Base

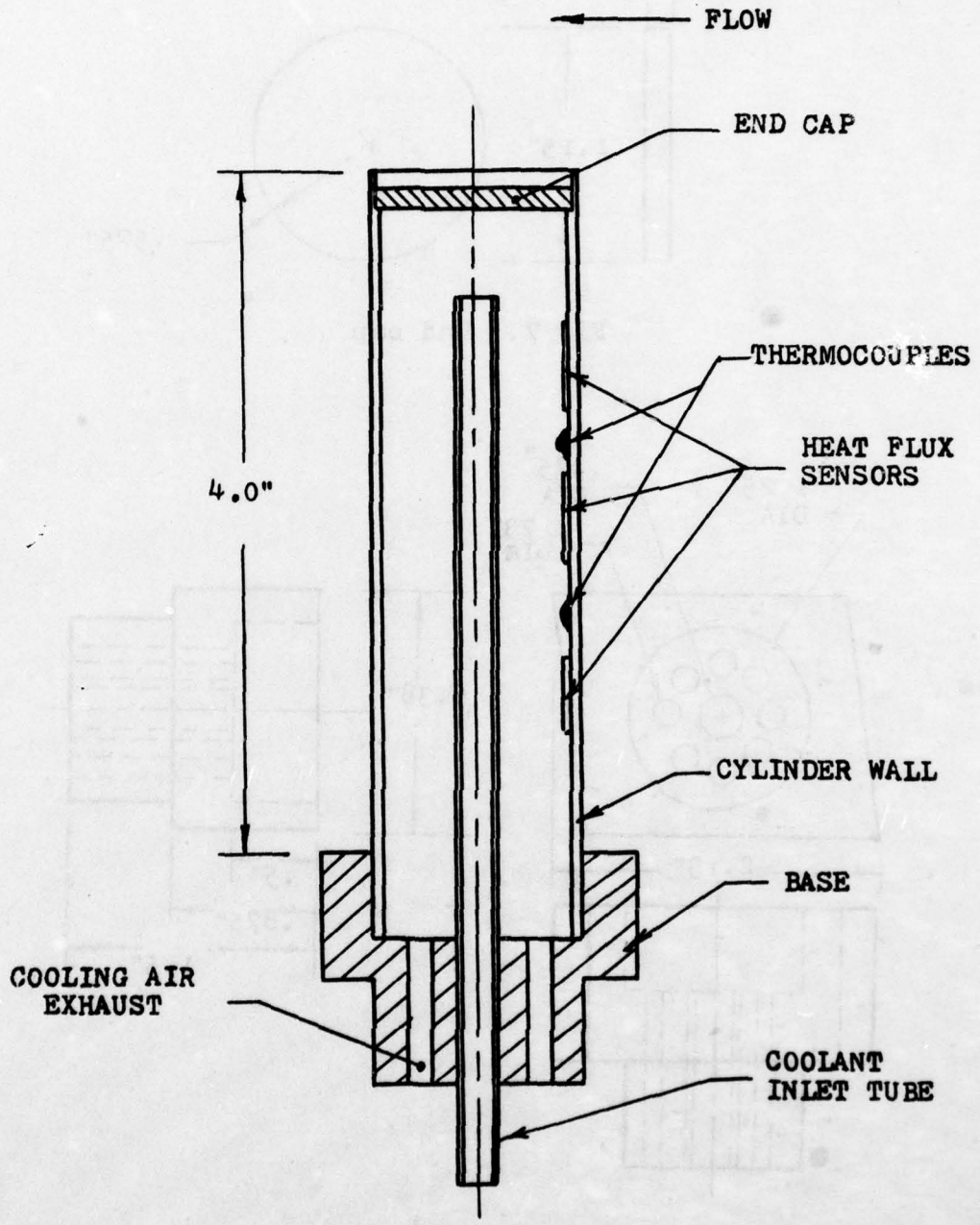

Fig 9. Assembled cylinder, base, and end cap (Cross section)

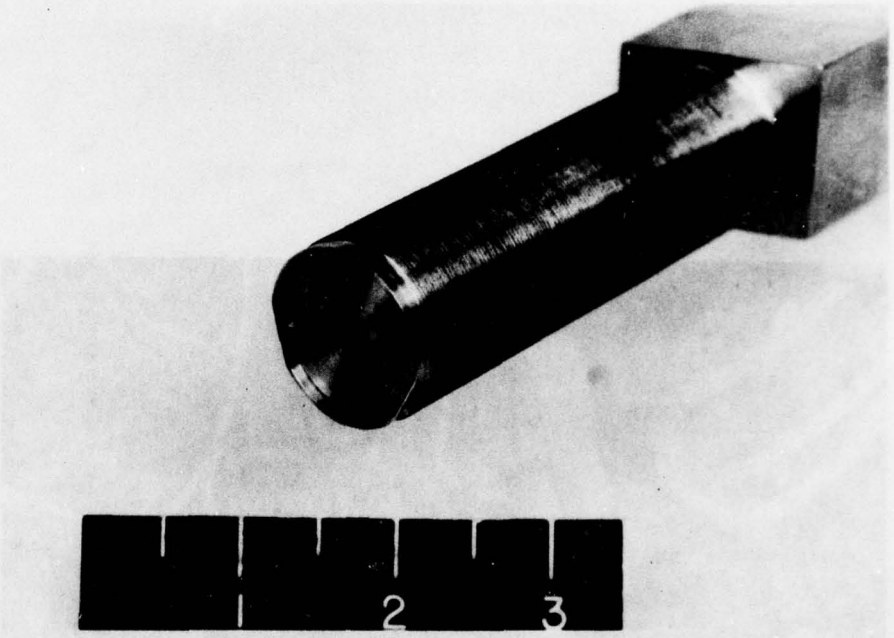

Fig 10. Threaded cylinder

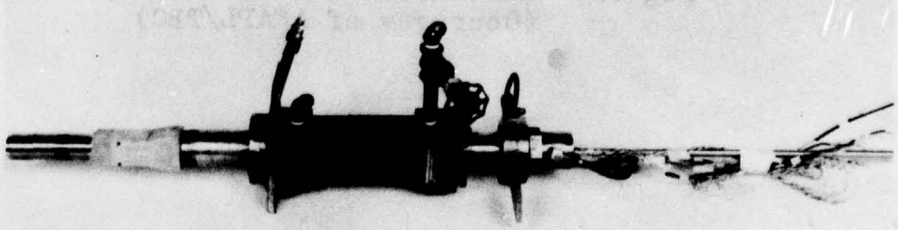

Fig 11. Threaded cylinder and actuator

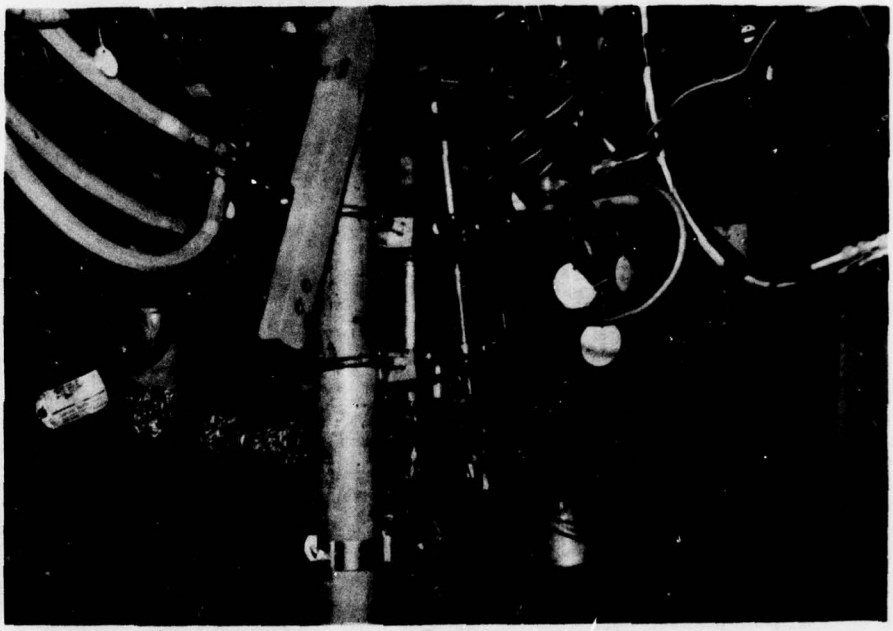

Fig 12. Installed actuator
(Courtesy of AFAPL/TBC)

Instrumentation

The inner wall of the cylinder at the stagnation line was instrumented with thermocouples and heat flux sensors as shown in Figure 13. The three Micro-foil heat flux sensors, serial numbers 429, 431 and 432, were obtained from RdF Corporation, Hudson, New Hampshire. Table 1 shows the nominal specifications for a sensor, part number 20450-1.

The sensors require no special wiring, reference junction or signal conditioning. The microvolt output is directly translatable to a heat flux of BTU/hr-ft^2. The three sensors were calibrated at the factory to have an output of 0.020×10^{-6} volts per BTU/hr-ft^2 at 70 ^{o}F. A calibration table was provided by the RdF Corporation for operation at temperatures other than 70 ^{o}F. The output voltage signal was converted to BTU/hr-ft^2 and was then multiplied by the appropriate factor from the calibration table to obtain the true heat flux. The specific equations used are shown in Section IV. Only the output from the center sensor was used in the calculation of heat flux. The data from the top and bottom sensors were compared to the center sensor output for a determination of accuracy.

The heat flux sensors operate by forming a multijunction thermocouple across a material of known thickness which becomes the thermal barrier. Figure 14 shows the typical construction of a heat flux sensor (Ref 8). As

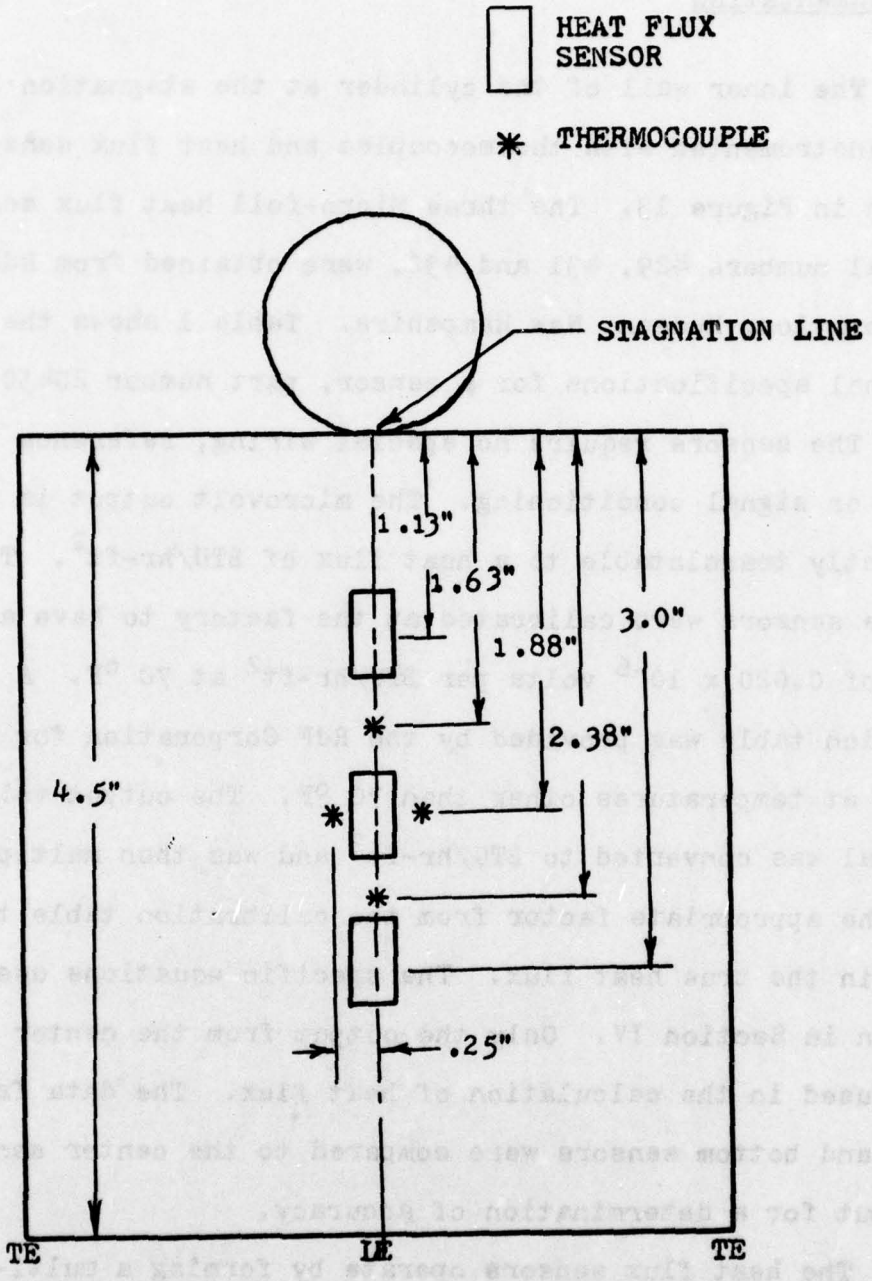

Fig 13. Instrumentation of cylinder (viewing inside surface)

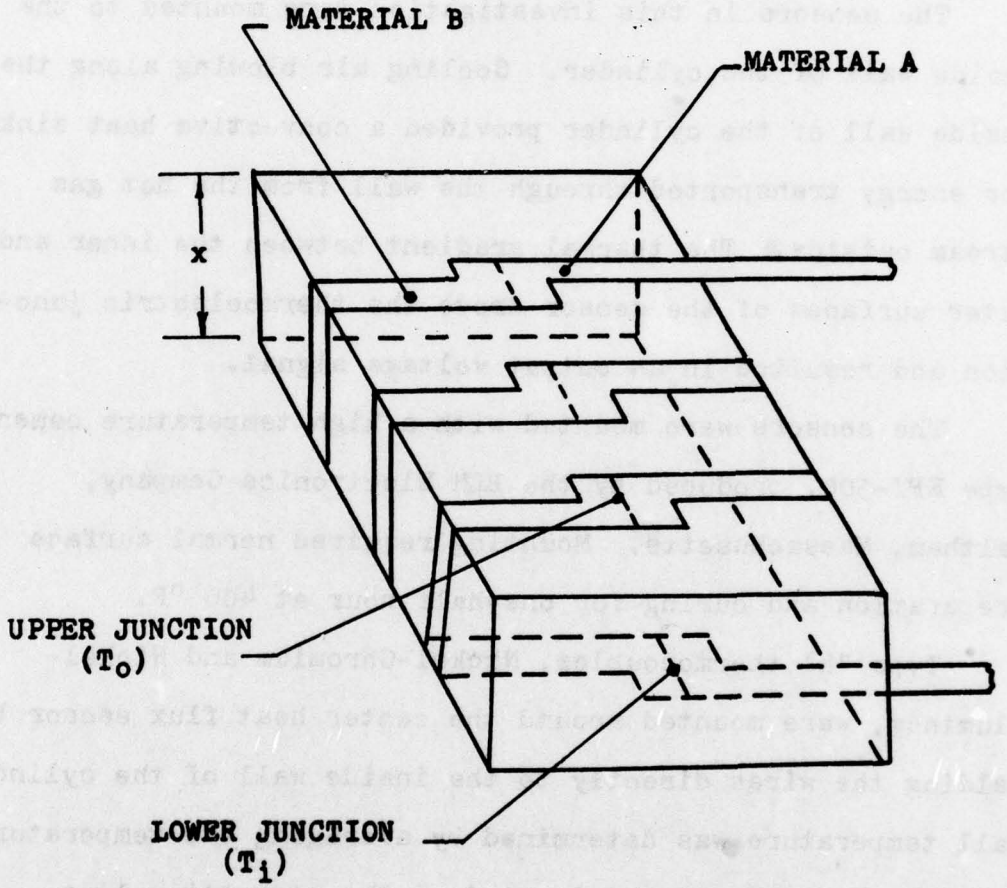

Fig 14. Heat flux sensor construction (Ref 8)

shown, multiple thermocouple junctions are used which give a stronger signal and greater sensitivity than a single junction.

The sensors in this investigation were mounted to the inside wall of the cylinder. Cooling air blowing along the inside wall of the cylinder provided a convective heat sink for energy transported through the wall from the hot gas stream outside. The thermal gradient between the inner and outer surfaces of the sensor drove the thermoelectric junction and resulted in an output voltage signal.

The sensors were mounted with a high temperature cement, type EPY-500, produced by the BLH Electronics Company, Waltham, Massachusetts. Mounting required normal surface preparation and curing for one-half hour at 400 ^{o}F.

Type "k" thermocouples, Nickel-Chromium and Nickel-Aluminum, were mounted around the center heat flux sensor by welding the wires directly to the inside wall of the cylinder. Wall temperature was determined by averaging the temperatures of the two thermocouples located on the stagnation line. Leads from thermocouples and sensors were tack-welded or potted to the wall with a Silicon compound (RTV). In addition to wall temperatures, cooling air temperatures were monitored by thermocouples mounted near the tip of the cooling tube and near the exit holes.

Gas stream temperatures were measured with a double-

shielded, water-cooled, type "R" thermocouple probe made of Platinum and Platinum-13% Rhodium. The probe was mounted on a traversing mechanism which enabled temperature readings to be taken directly in the center of the flow path. The probe traversed horizontally and was located at the entrance to the test section nozzle.

An IBM 1800 computer system was connected to the test facility. This permitted the monitoring of the flow and the cylinder in real time. Data was stored on magnetic tape and referenced by a data set number which was generated by each automatic data acquisition in 2.4 second intervals. A utility computer program was written to retrieve the data and calculate the required parameters (i.e., Reynolds number and Nusselt number). The calculations are shown in Section IV. The utility program was also used to eliminate data sets taken when the cylinder was out of the gas stream or undergoing transient conditions. The program was used to scrutinize more than two thousand data sets.

The extremely low output of the heat flux sensors, 2.0×10^{-5} volts per 1000 BTU/hr-ft^2, required the use of signal amplifiers. Each sensor was connected by shielded cable to a Preston 8300-XWB wide-band floating differential amplifier. These amplifiers are ideally suited to instrumentation requiring high accuracy, low noise, and high input impedance. Also, the accuracy ($\pm$0.01% of full scale output)

and low noise (less than 3 microvolts RMS) are not affected by the length of the input cable (Ref 9). This permitted the amplifiers to be mounted in the control room, away from a potentially explosive environment.

Honeywell Electronix 17, 4-channel strip chart recorders were connected to the output leads of the top and middle heat flux sensors and two thermocouples on the cylinder wall. The records of temperature and heat flux were used to determine when steady conditions were attained and to prevent the sensors from exceeding their maximum rated temperature. The strip chart recorders were believed to be inaccurate as compared to the computer tape records and were not used in the data analysis. Figure 15 shows a schematic of the instrumentation routing and the data acquisition system.

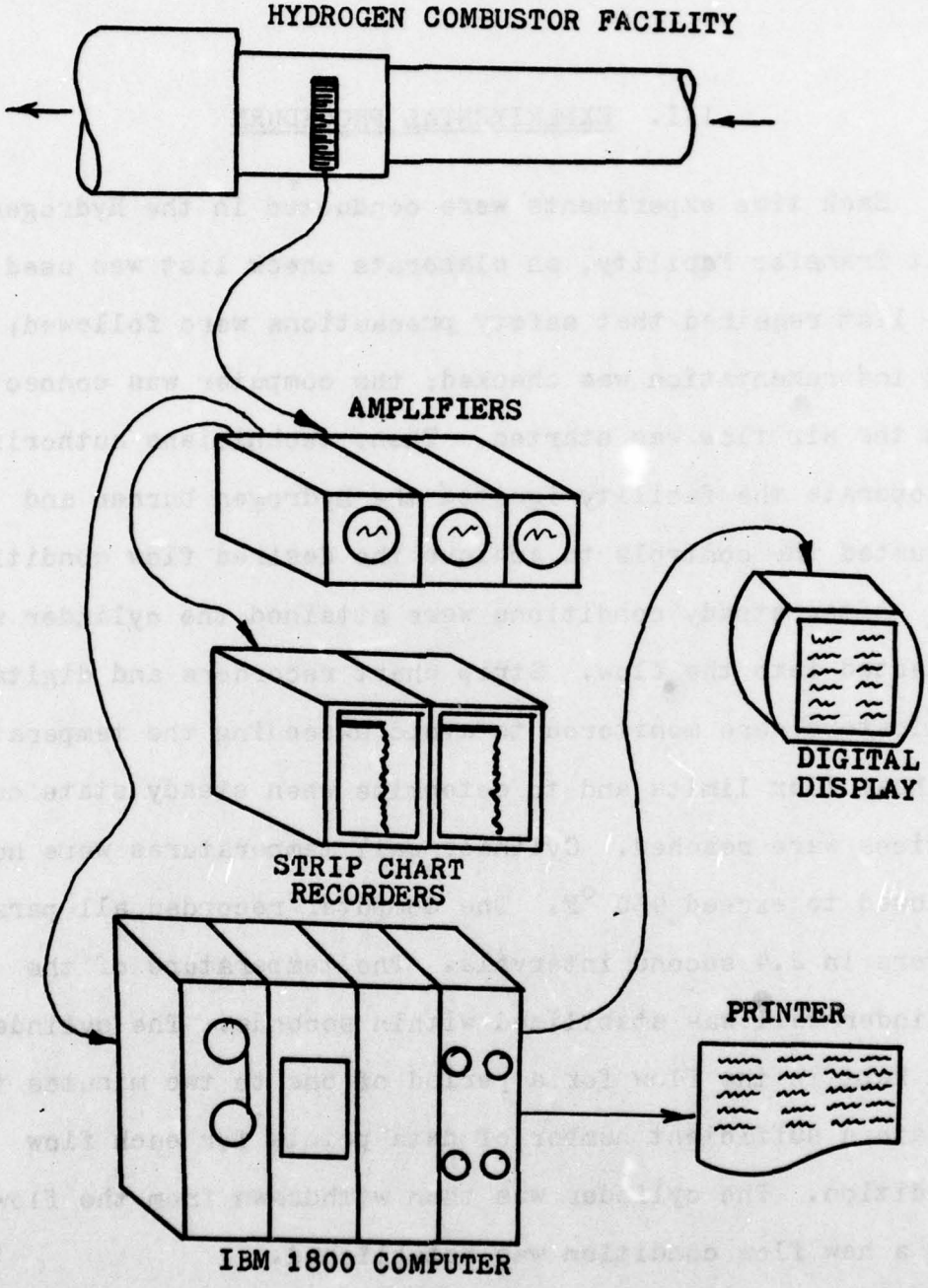

Fig 15. Instrumentation scheme

III. EXPERIMENTAL PROCEDURE

Each time experiments were conducted in the Hydrogen Heat Transfer Facility, an elaborate check list was used. The list required that safety precautions were followed; the instrumentation was checked; the computer was connected; and the air flow was started. Then, technicians authorized to operate the facility ignited the hydrogen burner and adjusted the controls to achieve the desired flow conditions.

After steady conditions were attained the cylinder was inserted into the flow. Strip chart recorders and digital indicators were monitored to avoid exceeding the temperature or heat flux limits and to determine when steady state conditions were reached. Cylinder wall temperatures were not allowed to exceed 450 ^{o}F. The computer recorded all parameters in 2.4 second intervals. The temperature of the cylinder wall was stabilized within seconds. The cylinder was kept in the flow for a period of one to two minutes to obtain a sufficient number of data points for each flow condition. The cylinder was then withdrawn from the flow and a new flow condition was established.

Data were recorded at Reynolds numbers (based on cylinder diameter) of 38,000 to 120,000. The number of flow

conditions achieved was limited by available test time because the test facility must share supply air with other test cells at AFAPL.

Cooling air during the test was maintained between 0.12 and 0.16 lbm/sec. Flow rates lower than 0.12 lbm/sec caused the cylinder wall temperature to rise above its limit. Flow rates greater than 0.16 lbm/sec caused the heat flux to exceed the scale of the recording equipment. Although the flow rate and the inlet and outlet temperatures were recorded, this information was not used because the data analysis did not require it.

After the threaded cylinder had been tested in a series of flow conditions, it was disconnected and removed from the combustor rig. The cylinder was then machined to remove only the threads while maintaining a wall thickness of 0.080 inches. The instrumentation was undisturbed during the machining and remained in the exact location of the previous tests. Following the machining, the cylinder was re-installed in the combustor rig.

Following the test procedure that was used for the threaded cylinder, the smooth cylinder was tested and data recorded on magnetic tape. The flow parameters achieved during the previous tests were repeated.

IV. RESULTS AND DISCUSSION

More than two thousand data sets were obtained during this investigation. Each data set included flow measurements (i.e., gas temperature, pressure, and mass flow rate) as well as test cylinder data (i.e., heat flux, wall temperatures, and coolant flow temperatures). The Reynolds number was calculated from the mass flow rate and temperature dependent dynamic viscosity, and was based on the cylinder diameter. Reynolds number is given by

$$Re_D = \frac{U_g D \rho}{\mu}$$

where

$$\rho U_g = \frac{\dot{m}}{A_t}$$

or

$$Re_D = \frac{\dot{m} D}{\mu A_t}$$

where

$$\frac{D}{A_t} = 0.8816 \text{ ft}^{-1} = \text{constant}$$

The interpolation of dynamic viscosity (Table 2) was based on bulk flow temperature which varied no more than 200 ^{o}F from the wall temperature (8% error in μ).

Nusselt number is determined by first evaluating the

heat flux, q, and then, the convective coefficient, h_g, of the outside wall. The heat flux is given by

$$q = 500(HF)(HFCF)$$

where the input from the heat flux sensor, HF, is in millivolts and HFCF is the sensor correction factor for use with varying surface temperature. Table 3 gives the correction factors, supplied by the manufacturer, which were computer interpolated and multiplied by the indicated heat flux to obtain the true heat flux measurement.

Assuming a one-dimensional heat flux, simultaneous equations can be solved for the convective coefficient as follows:

$$q_{cond} = \frac{k_w (T_{w,o} - T_{w,i})}{x}$$

$$q_{conv} = h (T_g - T_{w,o})$$

Assuming: $q_{cond} = q_{conv} = q$

$$T_g - T_{w,i} = q\left[\frac{x}{k_w} + \frac{1}{h}\right]$$

$$h = \left[\frac{(T_g - T_{w,i})}{q} - \frac{x}{k_w}\right]^{-1}$$

The conductivity, k_w, for 304 stainless steel varies with temperature as shown in Table 4.

Knowing h, the Nusselt number is given by $Nu = \frac{h D}{k_g}$

where k_g is also dependent upon gas temperature as shown in Table 5.

Using the equations shown above, the data reduction program calculated Reynolds number, convective coefficient, and Nusselt number for each steady state condition achieved. The data listed in Tables 6, 7 and 8 were taken from the steady state data sets. Table 6 lists the mean values and standard deviations of the calculated parameters at each flow condition for both smooth and threaded cylinders. These data have also been plotted on Figures 16 and 17. Figures 17 and 18 display the results from this study, laminar flow theory, the empirical relation presented by Dils and Follansbee (Ref 5), and data presented by Smith and Kuethe (Ref 3) for a turbulence intensity of 5%.

The plot of Nusselt number versus Reynolds number (Figure 17) shows large scatter for both the smooth cylinder and the threaded cylinder. The mean value of Nusselt number of the smooth cylinder climbed rapidly from Nu = 375 at Re_D = 34,750 to Nu = 620 at Re_D = 60,370. Between Re_D = 60,370 and Re_D = 80,400, the heat transfer was nearly constant, but then dropped to Nu = 452 at Re_D = 92,500. Beyond Re_D = 92,500, the Nusselt number increased, reaching Nu = 505 at Re_D = 104,300. No data were taken beyond Re_D = 104,300 for the smooth cylinder.

The threaded cylinder exhibited a different relation-

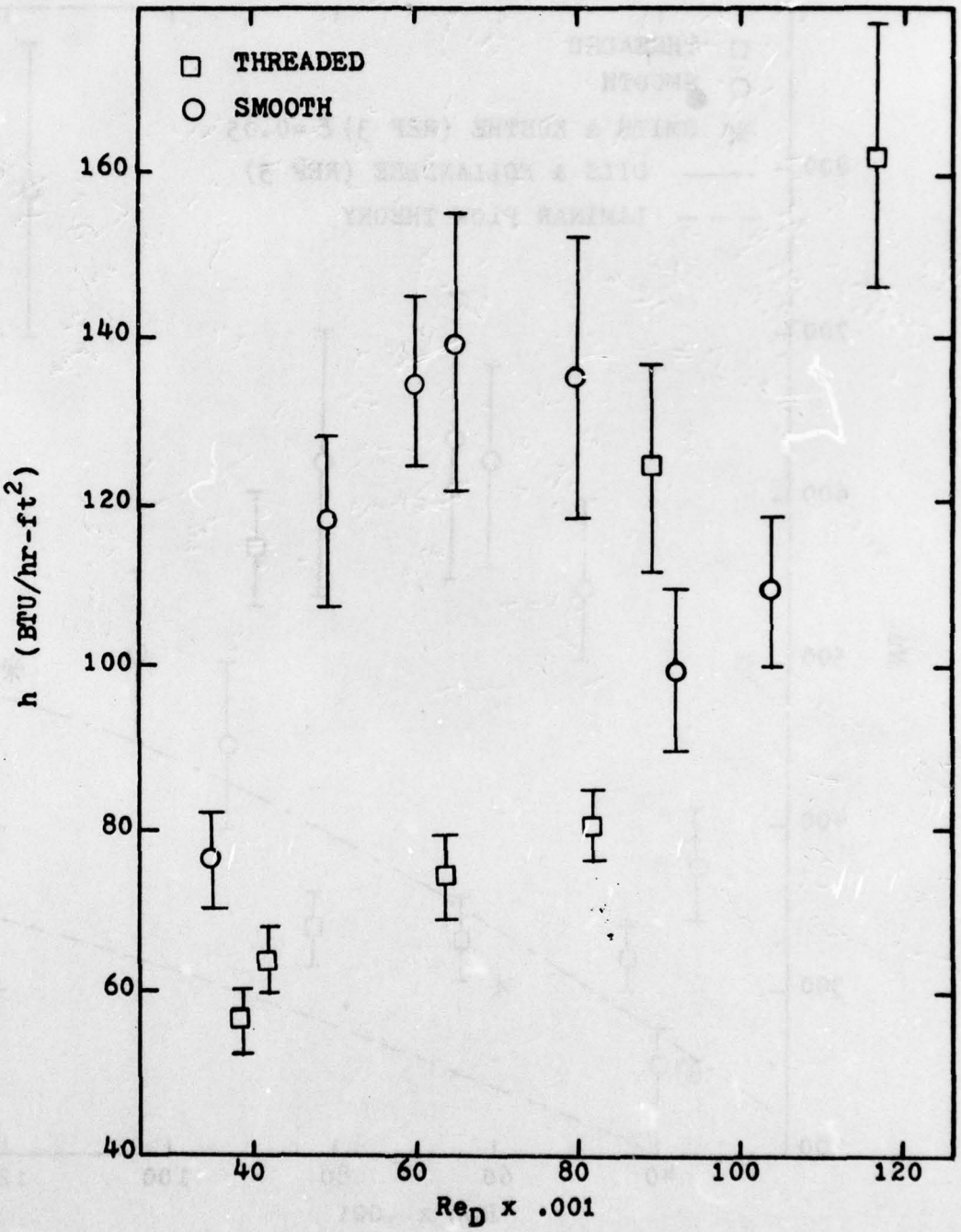

Fig 16. Stagnation line convective heat transfer coefficients (h) for cylinders in crossflow - mean value and standard deviation

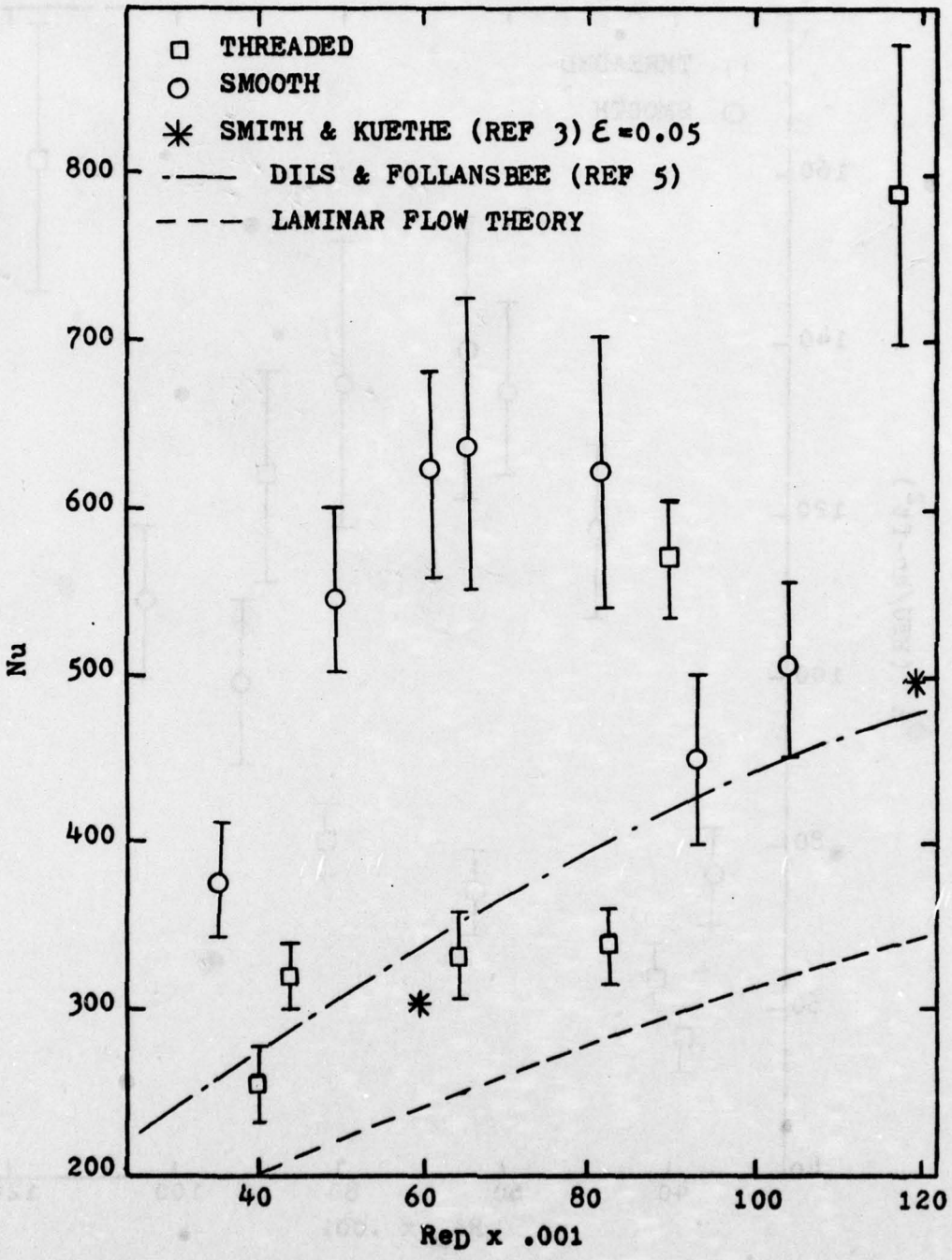

Fig 17. Stagnation line Nusselt number for cylinders in crossflow - mean value and standard deviation

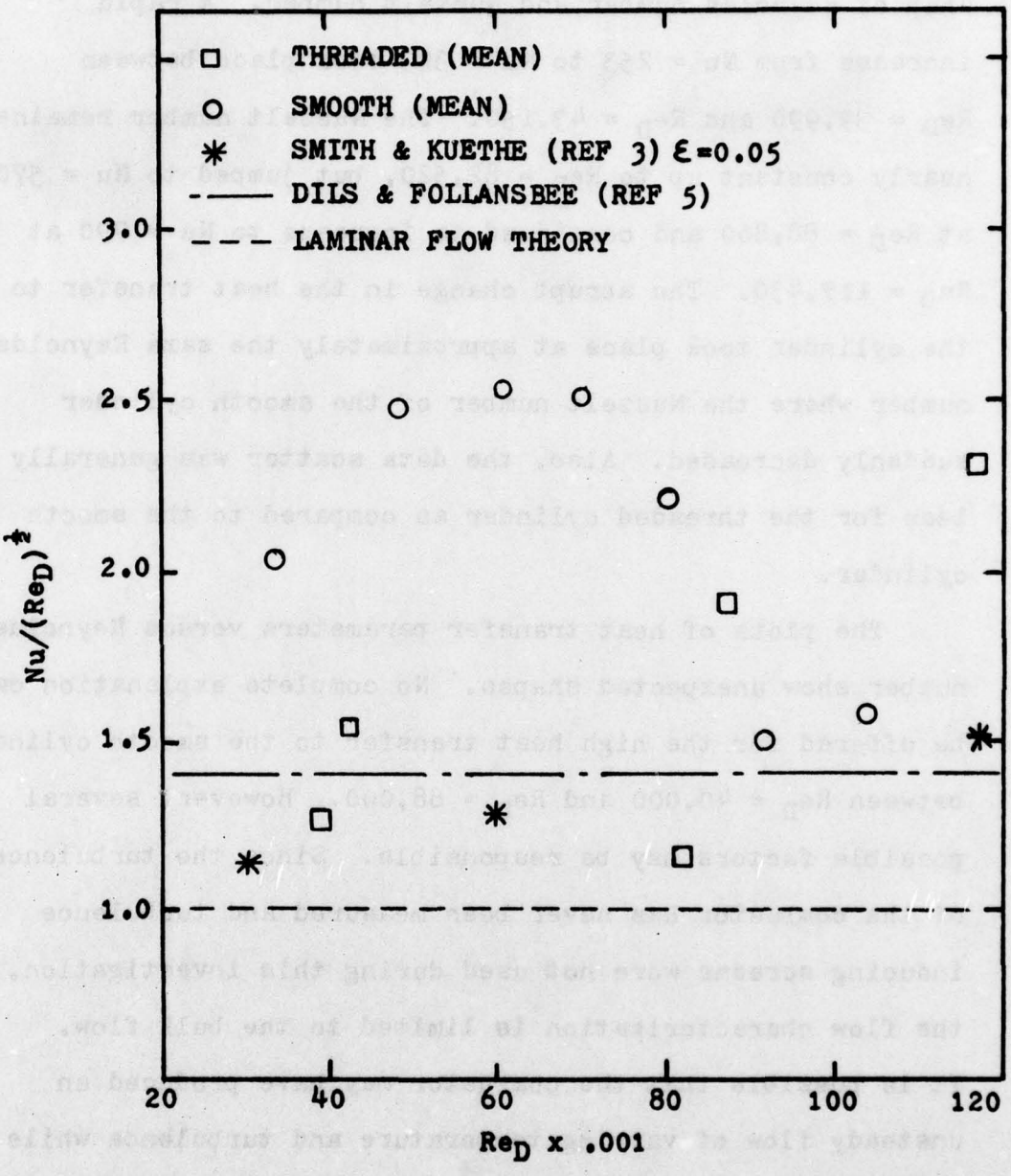

Fig 18. Heat transfer to the stagnation line of cylinders in crossflow

ship of Reynolds number and Nusselt number. A rapid increase from Nu = 253 to Nu = 323 took place between Re_D = 39,990 and Re_D = 43,150. The Nusselt number remained nearly constant up to Re_D = 82,520, but jumped to Nu = 570 at Re_D = 88,860 and continued to increase to Nu = 790 at Re_D = 117,430. The abrupt change in the heat transfer to the cylinder took place at approximately the same Reynolds number where the Nusselt number of the smooth cylinder suddenly decreased. Also, the data scatter was generally less for the threaded cylinder as compared to the smooth cylinder.

The plots of heat transfer parameters versus Reynolds number show unexpected shapes. No complete explanation can be offered for the high heat transfer to the smooth cylinder between Re_D = 40,000 and Re_D = 88,000. However, several possible factors may be responsible. Since the turbulence of the combustor has never been measured and turbulence inducing screens were not used during this investigation, the flow characterization is limited to the bulk flow. It is possible that the combustor may have produced an unsteady flow of varying temperature and turbulence while operating at temperatures below the minimum design temperature. The assumption of a uniform temperature profile was based upon previous measurements at higher temperatures (Ref 7). However, if the assumption that the same flow

conditions existed for both smooth and threaded cylinder tests is valid, then the threaded cylinder did not respond in the same manner as the smooth cylinder.

The rapid change in heat transfer between Re_D = 80,000 and Re_D = 90,000 may be due to the cylinder's boundary layer transitioning from laminar to turbulent flow. This transition has been documented for varying surface roughness (Ref 2:622) and takes place near Re_D = 10,000 for a cylinder in crossflow. Due to its increased kinetic energy, the turbulent boundary layer tends to remain attached to the cylinder wall longer and moves the separation point farther downstream. This would have a definite effect on the overall heat transfer to the cylinder by allowing hot turbulent gas to contact more of the cylinder wall. Heat transfer near the stagnation line may also be affected by this transition. This might explain the abrupt change of both the smooth and threaded cylinders at the same flow condition. Apparently, the threaded surface does not delay or enhance the transition.

Flow turning could possibly have had some effect. As shown previously (Figure 4), the nozzle was built to accept the flow from turbine vane airfoils. The free stream flow was assumed to be straight until it reached the cylinder. Some unexpected flow characteristic due to the downstream turning may have moved the stagnation line.

A large, general purpose computer program was used to model the threaded cylinder as a finned surface. The finite difference numerical analysis was necessary because the general equations derived in heat transfer texts are based upon assumptions of long, thin fins with a one-dimensional heat flow. Short fins have two-dimensional heat transfer.

The assumptions of

$$T_g = 910\ ^{o}R$$
$$T_{w,i} = 735\ ^{o}R$$
$$h = 100\ BTU/hr\text{-}ft^2\text{-}^{o}R$$
$$k_w = 10\ BTU/hr\text{-}ft\text{-}^{o}R$$

were used for mathematical models of the smooth and threaded surfaces. The analysis gave temperature profiles in two dimensions through the wall. The summation of the heat flows across an internal plane parallel to the surface determined the total heat flux entering the outer surface of the cylinder. This eliminated the need to consider two-dimensional effects at the threaded surface. The analysis predicted that the threaded surface would have a heat flux 1.55 times that of the smooth surface. The outer surface area of the threaded cylinder was 167% of the area of the smooth cylinder.

The data in Table 6 and Figure 16 show that the heat transfer to the threaded cylinder increases approximately

25% over that of the smooth cylinder at Re_D = 93,000. The data reflect only a portion of the predicted increase of 55%. Actual roughness effects may be completely hidden by the overall increase of heat transfer due to the finned surface. The data below Re_D = 93,000 do not agree with the prediction of the numerical analysis. In that flow regime, some facility-related effects may be dominate.

Measurement error was considered as a source of scatter. By noting the variation in recorded data, some estimate of each contribution to error can be determined. The calculated heat flux standard deviation was approximately 2% of the mean value for a given flow condition. This is comparable to a predicted accuracy of $\pm$ 2% for a type "K" thermocouple at a temperature between 300 ^{o}F and 500 ^{o}F.

The standard deviation of gas temperature as measured by the type "R" thermocouple was at or below 1.5% of the mean. The calculated gas stream pressure standard deviation was less than 0.25% of the mean. As mentioned previously, the amplifier error was $\pm$ 0.01%.

A sample data point was used to investigate the effect of combined errors for the worst case of individual errors. The following values for flow at Re_D = 114,000 were used in the equation for convective coefficient at the outer wall:

$$T_g = 920\ ^{o}R$$

$$T_{w,i} = 766\ ^{o}R$$

$$q = 15{,}900\ BTU/hr\text{-}ft^2$$

$$x = 0.00667\ ft$$

$$k_w = 10\ BTU/hr\text{-}ft\text{-}^{o}R$$

then $$h = \left[\frac{(T_g - T_{w,i})}{q} - \frac{x}{k_w}\right]^{-1} = 111\ BTU/hr\text{-}ft^2$$

Convective heat transfer coefficient was relatively insensitive to changes in wall conductivity. An error of 20% caused less than a 1% change in h. However, increasing gas temperature by 2% and decreasing wall temperature and heat flux by 2% resulted in h = 88 BTU/hr-ft^2 (21% decrease). Decreasing gas temperature by 2% and increasing wall temperature and heat flux by 2% resulted in h = 127 BTU/hr-ft^2 (14% increase). Both extremes are outside the data scatter presented on Figure 16. Clearly, the accumulation of small errors can be responsible for much of the data scatter.

V. CONCLUSIONS AND RECOMMENDATIONS

Conclusions

The results of this investigation lead to the following conclusions:

1. The Nusselt number - Reynolds number relationship of a threaded cylinder, measured on the stagnation line of the cylinder in crossflow (Re_d = 38,000 to 118,000), differs significantly from the response of a similar cylinder with a smooth surface. For Reynolds numbers less than 83,000, the smooth cylinder has a surface heat flux approximately 80% higher than that of the threaded cylinder. For Reynolds numbers above 88,000, the threaded cylinder has a heat flux 25% to 35% greater than the smooth cylinder.

2. Both the smooth and the threaded cylinders show a transition in heat flux between Re_D = 80,000 and Re_D = 90,000. This may correspond to the development of a turbulent boundary layer.

3. Assumptions about the flow conditions are very influential in the interpretation of the results. Using the test facility at temperatures below its designed operating temperature and at low mass flow rates may have resulted in unexpected temperature gradients in the flow

cross section. This may be responsible for the high heat flux to the smooth cylinder at Reynolds numbers less than 82,000.

4. Further investigation is needed to determine how the response of the cylinders may apply to the laminated airfoil. However, the present data show that the Reynolds number determines whether the heat flux is greater for the smooth surfaced airfoil or for the unfinished laminated airfoil.

Recommendations

The following are recommendations based upon this investigation:

1. Additional studies should be done to verify and better understand the unexpected Nusselt number - Reynolds number relationships for threaded and smooth cylinders in crossflow. This should include testing in a more predictable, simplified flow.

2. The turbulence intensity and temperature profiles should be characterized in the AFAPL test facility. The information would be useful in the interpretation of the results of this investigation. These studies could be accomplished jointly by an O.S.U. graduate student and AFAPL/TBC.

3. A full scale, laminated turbine vane should be tested in the AFAPL Hydrogen Heat Transfer Facility at the normal operating temperature. Smooth and threaded surface temperatures should be compared by the use of infrared photography.

TABLE 1 RDF Micro-foil heat flow sensor nominal specifications

Sensor size	.010 x .010 inch
Nominal Sensitivity	0.07 MV/BTU-ft^2-sec
Maximum Recommended Heat Flux	50 BTU/ft^2-sec
Response Time	0.02 seconds
Sensor Resistance	5 Ohm Maximum
Maximum Operating Temperature	500°F
Nominal Thickness	.003 inches
Thermal Capacitance	0.01 BTU/ft^2-°F
Thermal Impedance	0.003 °F/BTU-ft^2 hr

TABLE 2 Temperature dependence of dynamic viscosity of air

T (°R)	760	860	960	1060
$\frac{lbm}{ft\ sec}$	$1.61 \cdot 10^{-5}$	$1.75 \cdot 10^{-5}$	$1.89 \cdot 10^{-5}$	$2.0 \cdot 10^{-5}$

TABLE 3 Heat flux sensor correction factors

T (°R)	535	610	660	710	760	810	860	910	960
HFCF	1.0	.90	.84	.80	.76	.73	.70	.67	.65

TABLE 4 Temperature dependence of conductivity of 304 stainless steel

T (^{o}R)	672	1392
k_w (BTU/hr-ft-^{o}R)	9.4	12.4

TABLE 5 Temperature dependence of conductivity of air

T (^{o}R)	760	860	960	1060	1160	1260
k_w (BTU/hr-ft-^{o}R) x 100	1.93	2.12	2.31	2.50	2.68	2.86

Table 6 Stagnation line heat transfer for cylinders in crossflow - mean values and standard deviations from test data

# POINTS	$\overline{Re_D}$	s_{Re}	$\overline{Nu}$	s_{Nu}	$\overline{h}$	s_h
		SMOOTH SURFACE				
30	34754	470	375	30	76	6
30	49282	636	549	48	117	10
30	60370	747	620	58	134	11
38	65356	756	638	88	138	17
35	80443	958	621	83	135	17
34	92539	1148	452	49	99	10
40	104320	1409	505	46	109	9
		THREADED SURFACE				
25	39992	783	253	21	56	4
20	42247	631	310	12	64	4
35	43152	682	323	21	65	4
30	64981	1151	332	28	74	5
16	82515	715	336	21	80	4
25	88856	1088	570	64	124	13
23	117428	1108	790	88	162	16

Table 7 Typical values of stagnation line heat transfer coefficients for threaded cylinders in crossflow

Mach #	Re_D	h_{wall} BTU/hr-ft^2-^oR	Nu	T_g ^oR
.10	43600	70	347	825
.10	43400	67	335	835
.10	43300	67	329	835
.10	41600	63	304	865
.10	42400	65	312	860
.10	41600	61	292	875
.10	38800	54	239	953
.10	40200	56	254	936
.16	65700	78	357	928
.17	64800	71	313	959
.18	64200	69	301	978
.17	65300	71	317	949
.23	83000	81	342	1023
.22	88500	112	507	940
.21	89400	136	629	913
.21	90800	154	715	908
.22	87700	114	510	945
.24	118,500	188	926	839
.25	115,800	134	669	868
.25	116,400	152	737	859
.25	116,600	142	690	856

Table 8 Typical values of stagnation line heat transfer coefficients for smooth cylinders in crossflow

Mach #	Re_D	h_{wall} BTU/hr-ft^2-^oF	Nu	T_g ^oR
.24	102500	109	500	924
.25	101900	97	437	938
.24	105100	118	548	906
.24	106200	114	536	897
.23	92800	102	461	932
.23	91400	95	431	937
.23	91000	85	378	949
.20	80100	130	589	936
.20	80100	146	673	915
.17	64800	119	539	931
.17	65900	147	679	910
.17	64500	107	483	941
.17	66400	144	669	906
.16	61500	152	712	898
.16	59900	120	550	924
.15	59500	144	671	903
.13	50000	116	544	900
.13	49000	124	586	885
.13	50000	118	552	900
.13	49000	126	590	894
.09	35100	81	403	829

REFERENCES

1. Owen, P.R. and W.R. Thomson, "Heat Transfer Across Rough Surfaces," JOURNAL OF FLUID MECHANICS, Vol. 15, 1963.

2. Schlichting, H., BOUNDARY-LAYER THEORY, New York: McGraw-Hill Book Company, 1968.

3. Smith, M.C and A.M. Kuethe, "Effects of Turbulence on Laminar Skin Friction and Heat Transfer," PHYSICS OF FLUIDS, Vol. 9, No. 12, December, 1966.

4. Kestin, J. and P.F. Maeder, "Influence of Turbulence on Transfer of Heat from Cylinders," NACA Technical Note 4018, Langley Field, Virginia, 1956.

5. Dils, R.R. and P.S. Follansbee, "Heat Transfer Coefficients Around Cylinders in Crossflow in Combustor Exhaust Gases," Pratt & Whitney Aircraft Group, East Hartford, Connecticut, 1977, (ASME #77-GT-9).

6. Quick, D.H.; Henderson, R.E. and Tall, W.A., "Experimental Cold-Flow Investigation of Chordwise Static Pressure Distribution Around a Turbine Airfoil." AFAPL-TR-67-147, Wright-Patterson Air Force Base, March, 1968.

7. Vonada, J.A., "A Thermal Investigation of the AFAPL Turbine Engine Heat Transfer Test Facility," AFIT, Wright-Patterson Air Force Base, December, 1974.

8. "Micro-Foil Heat Flow Sensors," RdF Corporation data sheet 36614, Hudson, New Hampshire, 1977.

9. "Instruction Manual, Model 8300-XWB, Floating Differential Amplifier," Preston Scientific Incorporated, Anaheim, California, 1977.

*U.S.Government Printing Office: 1978 — 757-080/729